New & Renewable Energy 2025. 6 Vol. 21, No. 2
ISSN 1738-3935 (Print)
ISSN 2713-9999 (Online)
https://doi.org/10.7849/ksnre.2025.0015
[2025-6-WD-007]

Check for updates

Assessing Accuracy of Thrust-Curve-Based Models for Mooring Load Prediction in Floating Wind Systems

Ho-Seong Yang[1] · Ali Alkhabbaz[2] · Young-Ho Lee[3]*

Received 11 April 2025 **Revised** 12 May 2025 **Accepted** 10 June 2025 **Published online** 23 June 2025

ABSTRACT The accurate prediction of mooring line loads in floating offshore wind systems is critical for conducting design. These loads are significantly affected by the turbine thrust performance, which is typically governed by detailed turbine specifications such as blade geometry and control logic. However, such data are typically inaccessible owing to confidentiality, thus rendering thrust-curve-based simplified models a practical alternative. This study evaluates the reliability of a thrust-curve-based simplified model using only thrust curves, by comparing it with a fully detailed model that includes aerodynamic effects and controller logic. Both models are based on the IEA 15 MW reference turbine and the UMaine VolturnUS-S platform, and simulations were conducted under DLC 1.2 conditions using OrcaFlex. The results show that the simplified model estimates the rotor thrust and peak mooring loads within approximately 2% of those of the detailed model, thus demonstrating sufficient accuracy for early-stage design. However, in certain frequency bands, the simplified model shows higher responses owing to inadequate control-based load attenuation This study suggests that thrust- curve-based models can serve as a practical tool for mooring system design when turbine data are limited while highlighting the necessity for caution in fatigue-sensitive or high-fidelity applications.

Key words Floating offshore wind turbine(부유식해상풍력), Mooring system design(계류시스템설계), Thrust curve modeling(추력곡선설계), Load analysis(하중해석), Simplified model(간략화모델)

Subscript

BEM : blade element momentum

DLC : design load case

1) Doctor, Center for Offshore wind and Green hydrogen Ammonia Research, Korea Maritime and Ocean University, Busan, Korea

2) Doctor, Sustainable Energy Engineering Department, College of Engineering, University of Mosul, Mosul, Iraq

3) Research chair professor, Center for Offshore Wind and Green Hydrogen Ammonia Research, Korea Maritime and Ocean University, Busan, Korea

***Corresponding author:** lyh@kmou.ac.kr
Tel: +82-51-410-4940

1. Introduction

In recent years, global interest in offshore wind power has surged, driven by strengthened policies aimed at expanding renewable energy and achieving carbon neutrality.[1,2] In deep waters, where bottom-fixed structures are economically less viable, floating wind turbines have emerged as a promising alternative.[3,4] These floating systems offer greater flexibility in site selection compared to fixed structures, thus maximizing the potential of offshore wind resources.[5]

As a result, the demand for advanced design and analysis techniques for floating wind systems has grown, leading to the development and validation of

various numerical modeling approaches.[6,7] Floating wind turbines are inherently complex multi-degree-of-freedom dynamic systems, influenced by the coupled interactions of wind loads, waves, currents, and platform motions. Accurate simulations require integrated models that account for the turbine, tower, floating platform, and mooring system.[8,9]

In particular, precise prediction of extreme loads on mooring lines is critical in mooring system design, and these loads are highly sensitive to the turbine's thrust response characteristics. Detailed turbine information such as blade geometry, aerodynamic coefficients, and controller logic is therefore essential. However, in practical scenarios, this information is often unavailable due to confidentiality restrictions, limiting the ability to construct fully detailed models.[3,8] To overcome this limitation, simplified models that use thrust curves as a function of wind speed are commonly employed. These methods are supported by tools such as FAST and OpenFAST,[10,11] and serve as practical alternatives during early-stage design or when turbine data is limited.[3,12]

Numerous studies have explored the modeling and analysis of floating wind systems. Jonkman[3] laid the groundwork for dynamic modeling and load analysis, while Robertson *et al.*[13] evaluated the impact of mooring model fidelity on system response. Simplified modeling techniques have also been studied for instance, Truong & Ahn[14] assessed linear models against OpenFAST, and Pegalajar-Jurado & Bredmose[15] as well as Bachynski & Moan[16] analyzed response variations across different model complexities. Other works have compared power production and dynamic response,[17] or experimentally analyzed surge induced thrust variations,[18] confirming quasi-steady behavior in low frequency regions.

However, most prior research has focused on either a single modeling approach or mooring load estimation alone, and few studies have quantitatively compared thrust curve-based simplified models with fully detailed turbine models across the entire system response.

Such validation remains essential, especially because the dynamic response of the floating structure and turbine directly influences mooring loads. Without detailed modeling including controller effects and aerodynamic deformations simplified models may introduce significant errors in mooring response predictions.[8,12,19]

Therefore, this study constructs two models of the IEA 15 MW reference wind turbine[20] on the UMaine VolturnUS-S semi submersible platform:[21] one detailed model including aerodynamic and control system features, and one simplified model using only a thrust curve as input. Under the international design condition DLC 1.2,[22] the rotor thrust and mooring load responses of both models are quantitatively compared. The goal is to assess whether the simplified model can reliably predict peak mooring loads during early design stages when detailed turbine data is unavailable, and to provide foundational insights for future expansion into broader design scenarios.

While load cases such as DLC 6.x represent more extreme environmental conditions and may induce higher mooring tensions, this study focused on an initial feasibility assessment of the simplified model. Therefore, DLC 1.2 featuring rated wind speed and moderate wave loading was selected as it represents a typical operational condition where the turbine is actively controlled and thrust based loading is most meaningful. This choice allows for a focused evaluation of the model's capability in replicating mooring loads under realistic but controlled conditions prior to application in more severe environments.

2. Analysis condition and simulation setup

To compare the response differences between a simplified model based on a thrust curve and a detailed model incorporating aerodynamic and control characteristics, two simulation models were constructed

under identical conditions and subjected to numerical analysis. The target system is based on the IEA 15 MW reference wind turbine[20] and the UMaine VolturnUS-S semi submersible platform. The main specifications for the floater, tower, and mooring system were modeled based on the publicly available documentation.[21]

The controller employed in this study, as referenced in,[21] is based on the open source ROSCO framework developed for the IEA 15 MW reference turbine. It incorporates a proportional integral controller for blade pitch regulation and a torque controller for generator power optimization. The primary role of the controller is to maintain the rated rotor speed by adjusting the blade pitch angle in response to wind speed variations. For floating platforms, the default control settings were tuned to mitigate platform pitch interactions by modifying the PI gains and introducing peak shaving behavior around the rated wind speed region. These modifications reduce the excitation of low frequency motions and enhance system stability under turbulent wind conditions. The controller operates in Region 2.5 of the wind turbine power curve, where active pitch control is crucial for load attenuation and rotor thrust regulation.

The simulations were conducted using OrcaFlex 11.3a, a commercial software widely used for analyzing nonlinear motions and mooring dynamics of offshore structures. The platform's six degrees of freedom motions and mooring responses were computed based on time domain simulations considering the time history of external loads. Hydrodynamic analysis employed the Response Amplitude Operator based on linear wave theory within OrcaFlex, accounting for wave added mass, damping, and wave excitation forces acting on the floater. Wave inputs were defined using the JONSWAP spectrum, and the mooring system was modeled as a three line catenary wire configuration in 200 meters of water depth, reflecting a realistic marine environment.

Aerodynamic analysis was performed using OrcaFlex's BEM module. Airfoil data were assigned to each blade section, and lift, drag, and moment coefficients were pre defined based on angle of attack. Major aerodynamic phenomena, including tip loss, skewed wake, and dynamic inflow effects, were included to enable real time calculation of rotor thrust and pitch moment over time. The model also supported aeroelastic coupling by incorporating blade geometry, stiffness, and mass distribution. The control system applied was based on the default torque and pitch controller settings defined in.[21] In contrast, the simplified model was configured under the same structural and environmental conditions, but with wind speed dependent thrust curves used as direct input. This model excluded aerodynamic and controller effects, and only computed the response of the mooring lines and floater accordingly.

In this study, the simplified model was constructed by generating time history thrust loads based on the wind conditions of DLC 1.2 and directly applying them as external forces to the floater, thereby simplifying the turbine representation. To maximize model simplicity, the calculation of wind speed acting on the turbine did not account for the relative velocity caused by the dynamic motion of the floater. Consequently, in floating offshore wind systems where significant platform motion occurs, applying thrust without considering this relative velocity can lead to discrepancies in the system's dynamic response. Furthermore, aerodynamic damping effects, which require detailed turbine specifications, were not included in the simplified model.

The key structural differences between the two models are illustrated in Fig. 1, and a detailed comparison of each component is provided in Table 1, allowing for a clear understanding of the modeling framework adopted in each case.

In addition, the specific simulation conditions including mean wind speed, turbulence intensity, and total simulation time are summarized in Table 2. These conditions were defined based on DLC 1.2, one of the

design load cases outlined in the international standard DNV-RP-C205,[22] in order to enable a direct comparison of wind induced response characteristics. The platform, tower, and mooring system configurations were kept identical for both the detailed and simplified models.

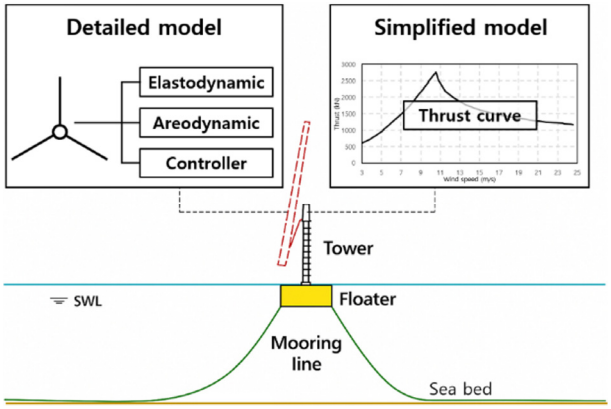

Fig. 1. Schematic diagram of the modeling strategy

Table 1. Configuration comparison between the detailed model and the simplified model

Component	Detailed model	Simplified model
Hydrodynamic modeling	BEM-based aerodyn	Thrust curve input
Control system	Pitch controller (DLL implementation)	N/A
Wind input	Identical turbulent time series (Turbsim)	
Floating platform	VolturnUS-S semi-submersible	
Mooring system	Three-line catenary mooring	
Simulation tool	Orcaflex	

Table 2. Simulation conditions for DLC 1.2

Parameter	Value
V_{hub} (avg.10 min)	10.59 m/s
wind shear	0.14
Wind model	NTM
turbulence intensity	14%
Hs (3 hr)	1.84 m
Tp	7.5 s
gamma	1
Wave model	NSS
Current	N/A
Water level	MSL, 0.207 m
Simulation time	3 hr

3. Validation of the simplified model

In the early stages of design, it is often difficult to obtain detailed aerodynamic data or control logic for wind turbines. As a result, simplified models that use wind speed dependent thrust curves are frequently adopted in practical engineering applications. While such models offer advantages in terms of simulation efficiency, their omission of actual aerodynamic and control system responses necessitates prior validation to ensure prediction reliability.

This section evaluates how closely the thrust curve-based simplified model replicates the response of a fully aerodynamic model under various mean wind speed conditions. The aim is to assess the degree of load prediction accuracy the simplified model can achieve within the design envelope, and to determine its quantitative applicability in subsequent simulation stages.

Before directly comparing the simplified model (based on thrust curve input) with the detailed model, a preliminary verification step was conducted to confirm that the detailed model itself adequately reproduces the turbine's design standards. Specifically, the thrust response calculated by the detailed model was compared to the official design thrust curve provided for the IEA 15 MW reference turbine. Fig. 2 presents this comparison across a range of wind speeds. A deviation was observed between 9 m/s and 12 m/s due to the influence of the controller implemented in this study, which resulted in peak shaving in the simulation. However, outside this range, the simulation results matched the design curve very closely. This confirms that the detailed model used in this study faithfully reproduces the turbine's design thrust data, and is therefore valid for use as a benchmark in the comparison with the simplified model.

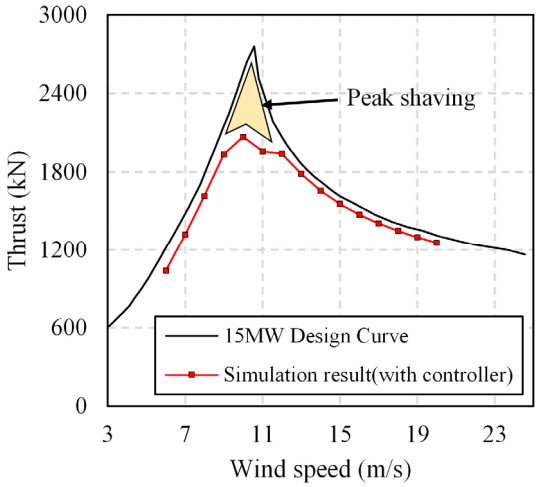

Fig. 2. Comparison between design thrust curve and simulation-derived thrust values from the detailed aerodynamic model

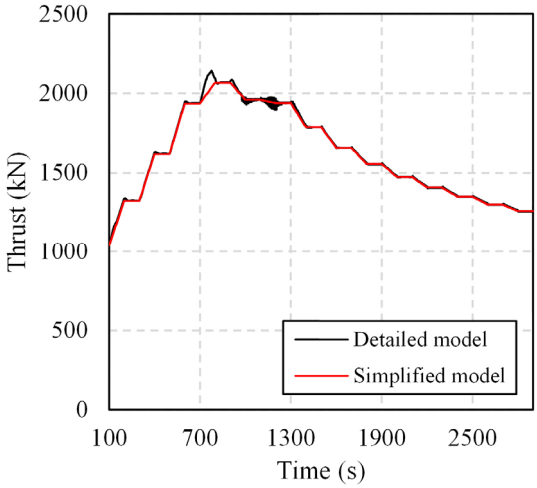

Fig. 3. Comparison of rotor thrust time histories for the simplified and detailed models

3.1 Time-series analysis

Based on the previous validation, this study constructed the input thrust curve for the simplified model not from the original design thrust curve of the IEA 15 MW turbine, but from the mean thrust values obtained from the detailed model simulations across various wind speeds. To enable real time application of thrust loads corresponding to varying wind speeds, a custom Python script was integrated using the External Function feature in OrcaFlex. This script receives wind speed as input, references a predefined wind speed thrust mapping table, and applies linear interpolation between wind speed intervals, allowing the thrust curve to be implemented as a continuous function rather than a discrete set of values.

To verify the validity of this simplified model configuration, a simulation was performed where wind speed was incrementally increased at fixed time intervals, as shown in Fig. 3. The initial wind speed was set to 6 m/s and was increased stepwise every 200 seconds up to 20 m/s, covering the range of 9 to 20 m/s in 1 m/s increments. This scenario was designed to quantitatively examine the thrust response characteristics of both models across the full design wind speed range.

The results show that the simplified model maintained a constant thrust value for each defined wind speed interval, while the detailed model exhibited sharp thrust variations and oscillatory responses near the rated wind speed due to controller actions and aerodynamic dynamics. Nevertheless, the overall thrust trend showed good agreement between the two models, indicating that the simplified model effectively approximates the thrust behavior of the 15 MW turbine.

Next, before conducting the full floating system analysis (including platform motion), the study investigated whether there are inherent structural differences in the rotor thrust response characteristics between the two models. As shown in Fig. 4, both models were simulated under the same DLC 1.2 wind conditions with the platform fixed, allowing comparison of the rotor thrust response while excluding platform motion. In this configuration, environmental disturbances such as wind and waves were kept identical, enabling a fair evaluation of how each model responds to the same wind field.

The results showed that the mean rotor thrust values both models were closely matched, with an average error of only −0.65%, as shown in Table 3. In addition,

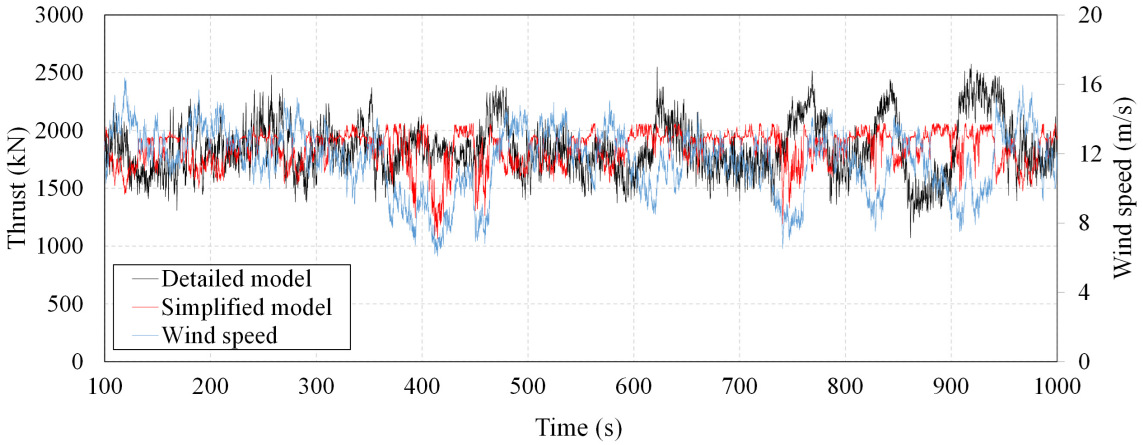

Fig. 4. Rotor thrust response comparison under fixed conditions (DLC 1.2 wind field, fixed)

Table 3. Comparison of fixed condition rotor thrust statistics between the detailed model and simplified model

Error metric	Value (%)
Mean rotor thrust	−0.65
Mean instantaneous thrust error	14.44
Std. deviation of instantaneous error	9.8

the mean instantaneous thrust error calculated as the average of absolute differences at each time step was 14.44%, indicating that although the average thrust levels are similar, local deviations are more pronounced. These deviations arise not because of increased fluctuation in the detailed model, but rather due to the difference in how each model responds to rapid wind changes. The simplified model reflects abrupt thrust changes directly from the input wind speed, whereas the detailed model moderates this behavior through pitch and torque control, aiming to maintain thrust stability. This difference in dynamic response characteristics between the models results in higher instantaneous thrust errors, especially during periods of fluctuating wind conditions.

Fig. 5 presents a scatter plot constructed from the full time series data obtained under DLC 1.2 conditions with the platform fixed. It maps the wind speed at each time step against the corresponding rotor thrust value. As seen in the figure, the simplified model

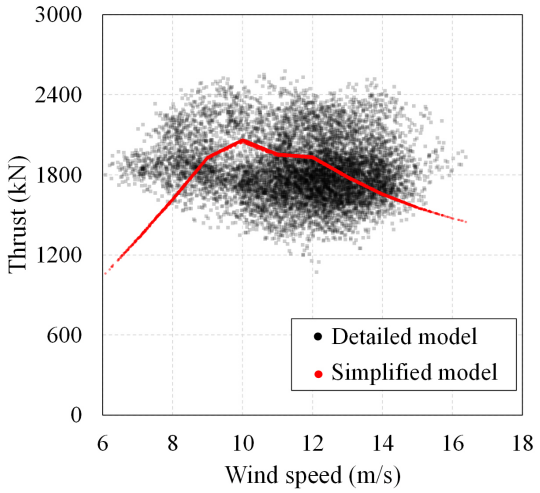

Fig. 5. Comparison of thrust response scatter for simplified and detailed models under DLC 1.2 (fixed condition)

closely follows the design thrust curve throughout the entire simulation period, demonstrating that the thrust table was accurately applied in response to real time wind speed variations.

In contrast, the detailed model also shows thrust responses that generally cluster near the design thrust curve. However, in regions with rapid wind speed fluctuations or near the rated wind speed range, deviations occur due to controller induced peak shaving or delays in aerodynamic and control system responses. These discrepancies reflect the complex dynamic behavior of the detailed model.

This trend becomes more pronounced in off-design wind speed ranges, particularly at lower wind speeds (6 to 9 m/s) and higher wind speeds (above 17 m/s), where the differences from the design curve increase. The results highlight that while the detailed model attempts to follow the design thrust curve as closely as possible through its aerodynamic and control mechanisms, it is inherently limited by system response delays and rapidly changing wind conditions, making perfect adherence to the design curve impractical.

4. Result

This section presents a quantitative comparison between the simplified thrust curve based model and the detailed model incorporating aerodynamic and control features as applied to a floating offshore wind turbine system. The simulations were conducted under DLC 1.2, and the comparison focuses on key response metrics including rotor thrust, mooring line tension, statistical load indicators, and frequency domain responses.

Fig. 6 illustrates the time series comparison of rotor thrust generated by the two models under DLC 1.2 conditions. Similar to the results observed in the fixed-platform simulations, the detailed model exhibited several high load instances that exceeded the design thrust curve, primarily due to turbulent wind speed fluctuations and dynamic controller responses such as pitch control. In contrast, the simplified model, which applies a fixed thrust input based on a wind speed dependent thrust table, showed a more constrained thrust response even under rapidly changing wind conditions, owing to the absence of dynamic aerodynamic or control feedback.

The quantitative comparison of thrust responses is summarized in Table 4. The mean rotor thrust calculated from the detailed model was 1,968.61 kN, while that of the simplified model was 1,877.02 kN, indicating a difference of approximately −4.65%. Additionally, the mean instantaneous error in the time-series thrust was about 12.01%, and the standard deviation of the instantaneous error was 9.2%, confirming that there is a significant difference in the variability of instantaneous responses between the two models.

Table 4. Comparison of rotor thrust statistics between the detailed model and simplified model

Error metric	Value (%)
Mean mooring tension	−4.65
Mean instantaneous mooring tension	12.01
Std. deviation of instantaneous error	9.27

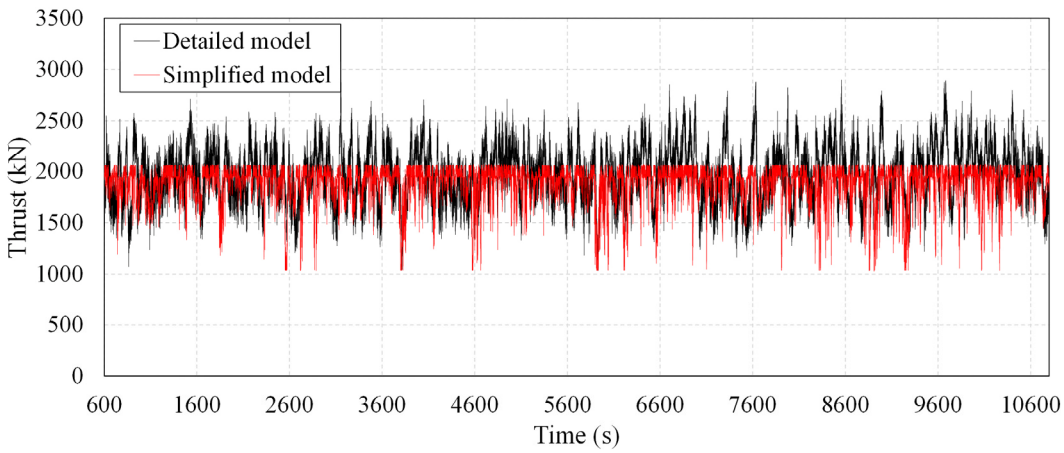

Fig. 6. Time-series comparison of rotor thrust between detailed model and simplified models (free condition)

Fig. 7 presents the time-series comparison of mooring line tension obtained from both models under DLC 1.2 conditions. This particular mooring line was selected because it is located on the windward (front-side) of the platform, where the influence of rotor thrust is most prominent.

Despite exhibiting different thrust response characteristics, both models produced similar maximum mooring loads, each exceeding 4,500 kN over the course of the 3 hour simulation. The figure also highlights the top 14 peak tension values recorded from each model. While the temporal distribution of these peak values varies between the models, the magnitude of the response remains comparable. Notably, the simplified model, despite lacking aerodynamic modeling and active control systems, still yielded tension responses that were not significantly different from those of the detailed model.

Although both models applied a nacelle tilt angle of 6 degrees, the way thrust loads were derived and applied differs fundamentally. In the detailed model, aerodynamic calculations naturally account for the inclined inflow due to the platform pitch and nacelle tilt, which leads to a reduced effective horizontal thrust component. In contrast, the simplified model uses pre-defined thrust curve values based on horizontal wind input and applies them with a tilt angle but without adjusting for the true inflow direction or its effect on horizontal loading. As a result, the horizontal component of the thrust tends to be overestimated in the simplified model, explaining the higher peak tensions observed in Fig. 7.

To enable a comparison of the mooring average tension responses between the models, Table 5 presents a statistical summary of the mooring loads shown in Figure 7. The mean mooring tension error was calculated to be 8.41%, indicating a slight overestimation by the simplified model. The mean instantaneous error was 10.81%, with a standard deviation of 7.86%, reflecting moderate variation in the amplitude of tension values between the two models.

Fig. 8 presents a comparison of the power spectral density (PSD) of mooring line tension for the two models under DLC 1.2 conditions. By converting the time domain responses into the frequency domain, the graph quantitatively illustrates how much energy each frequency component contributes to the mooring

Table 5. Comparison of mooring tension statistics between the detailed model and simplified model

Error metric	Value (%)
Mean rotor thrust	8.41
Mean instantaneous thrust error	10.81
Std. deviation of instantaneous error	7.86

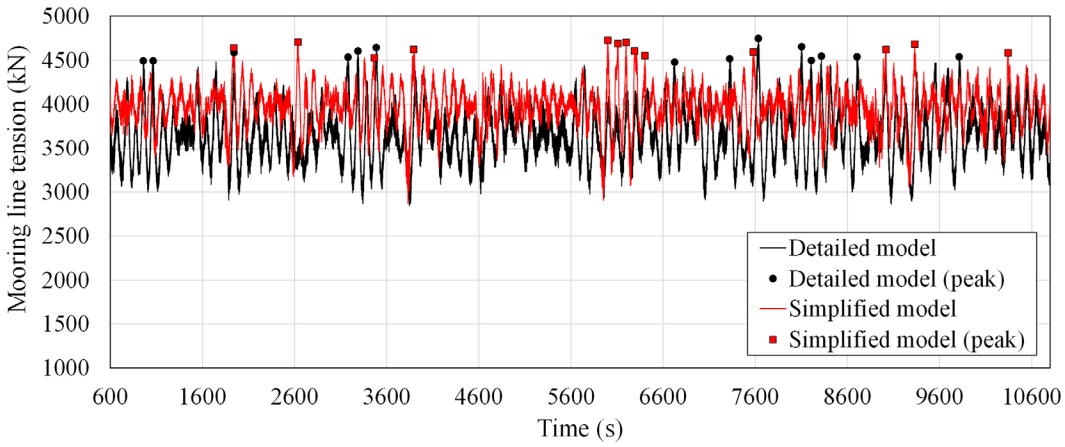

Fig. 7. Time history of mooring tension under DLC 1.2. Top 15 peaks from each model are marked

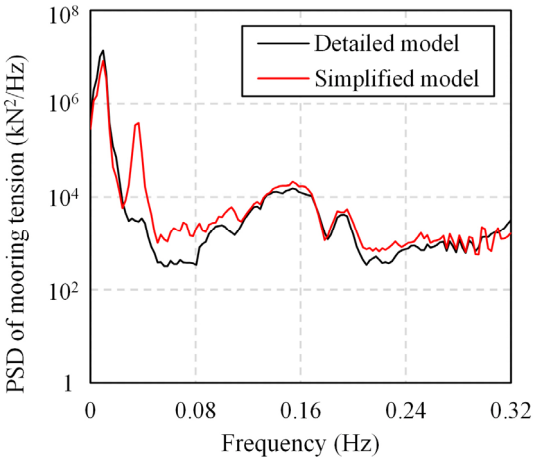

Fig. 8. Frequency domain analysis of mooring tension via FFT

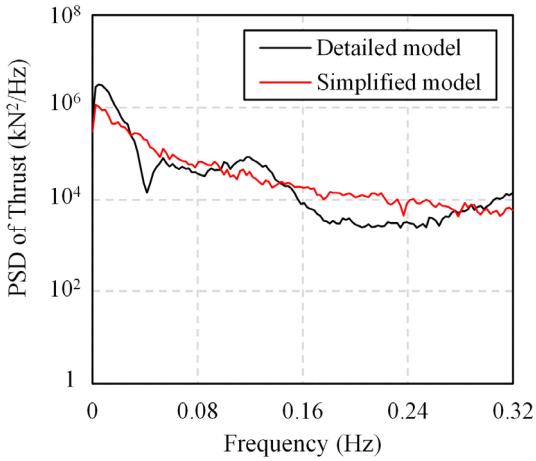

Fig. 9. Frequency domain analysis of rotor thrust via FFT

line loads. As shown in the figure, the simplified model exhibits a generally similar frequency response pattern compared to the detailed model, but shows higher PSD values in certain frequency bands. In particular, the simplified model shows a notably stronger response around 0.04 Hz, suggesting that it may overestimate thrust fluctuations or underrepresent damping effects in specific periodic responses. In the 0.1 to 0.2 Hz range, both models show comparable energy distributions. Overall, the simplified model successfully replicates the load distribution characteristics of the detailed model not only in terms of average response levels but also across major frequency components. However, some discrepancies are observed in specific natural frequency regions.

Fig. 9 compares the power spectral density of rotor thrust obtained under DLC 1.2 conditions. As shown in the graph, the simplified model produces higher PSD values near 0.04 Hz, indicating that thrust fluctuations in this low frequency offshore band are more pronounced. A notable difference between the two models appears around 0.04 Hz, as observed in both the mooring tension PSD and the rotor thrust PSD. This frequency corresponds to the natural pitch frequency of the floating platform. In the detailed model, the implemented pitch and torque control systems act to damp out oscillations around this resonance frequency by adjusting the blade pitch in response to platform motion and aerodynamic loading. As a result, the thrust variations and consequently the mooring line loads are effectively suppressed at this frequency.

In contrast, the simplified model lacks such control mechanisms and aerodynamic damping effects. Therefore, the pitch induced oscillations remain unattenuated and are directly transmitted as fluctuating thrust forces, leading to amplified mooring tension responses near 0.04 Hz. This explains the higher PSD values observed in the simplified model around this frequency range. This distinction is also considered one of the main factors behind the frequency domain differences observed earlier in the mooring line load responses.

Fig. 10 compares the top 14 peak tensions extracted from the time series mooring line response of mooring line under DLC 1.2 conditions. The figure visually illustrates the response differences between the two models for each individual peak. A detailed quantitative comparison of these values is provided in Table 6, which summarizes the absolute differences and relative error rates, enabling a comprehensive analysis of both the overall similarity and minor deviations between the models.

As shown in the figure, except for the first peak,

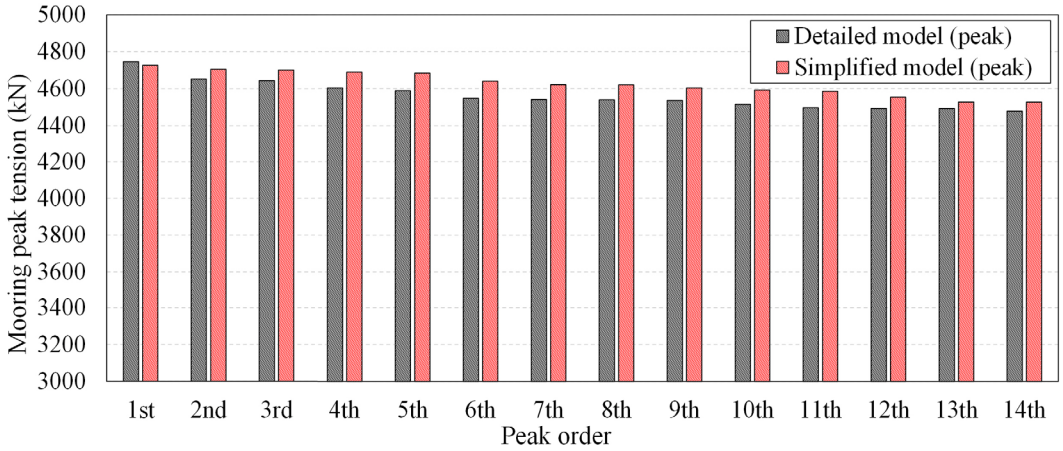

Fig. 10. Comparison of the top 14 peak mooring tensions under DLC 1.2

Table 6. Quantitative comparison of top 14 peak tensions in Mooring Line #1 under DLC 1.2

Peak	Difference (kN)	Error (%)
1st	−21.17	−0.45%
2nd	51.76	1.11%
3rd	56.82	1.22%
4th	84.58	1.84%
5th	95.06	2.07%
6th	93.28	2.05%
7th	80.77	1.78%
8th	81.27	1.79%
9th	67.43	1.49%
10th	75.63	1.67%
11th	86.72	1.93%
12th	58.85	1.31%
13th	33.48	0.75%
14th	47.24	1.05%

the simplified model generally exhibited slightly higher peak tensions than the detailed model across most cases. The maximum difference observed was approximately 95.06 kN (2.07%), and the overall range of error was within −0.45% to +2.07%, indicating a relatively narrow margin of variation.

This trend is attributed to the absence of instantaneous load damping in the simplified model, which lacks control system functionality. As a result, it does not reflect the load mitigation effects typically induced by active control responses. In particular, the amplified PSD of rotor thrust at 0.04 Hz observed in Fig. 9 is considered a key factor contributing to the increase in peak mooring tensions in the time domain. Although the first peak in the detailed model was higher than that of the simplified model, this is regarded as an anomalous case, likely caused by momentary wind fluctuations or timing differences in the controller's response. Overall, however, the magnitude of the peak tensions predicted by the simplified model closely matched those of the detailed model.

5. Conclusion and discussion

This study aimed to whether a simplified thrust curve based model can reliably predict peak mooring loads in a floating offshore wind turbine system even when detailed turbine specifications are not available an issue that commonly arises in practical mooring system design. Specifically, using the IEA 15 MW floating offshore wind system, a comparison was conducted between a detailed model that includes aerodynamic and control system features, and a simplified model based solely on wind speed dependent thrust curves. Both models were simulated under the same environmental conditions, and their responses in

terms of rotor thrust and mooring line tension were quantitatively analyzed.

The results showed that, despite the simplified model lacking aerodynamic and control dynamics, its overall rotor thrust and predicted peak mooring line load under DLC 1.2 were within approximately 2% of those from the detailed model. Moreover, in terms of extreme mooring tension magnitudes and rank distributions which are critical factors for mooring system design the differences between the two models were not significant. This confirms that the simplified model holds substantial potential as a practical alternative tool, particularly during early stage design or in data limited scenarios.

In addition to its predictive accuracy, the simplified model demonstrated a significant computational advantage. Under identical DLC 1.2 simulation settings, the detailed model required approximately 911 minutes for time domain simulation, whereas the simplified model completed the same in about 120 minutes a reduction by a factor of roughly 7.6. This level of efficiency is particularly beneficial in early stage design phases, parametric studies, or optimization tasks, where numerous simulations are often required. While the simplified model sacrifices some physical fidelity, its ability to deliver reasonably accurate results with much lower computational cost makes it a valuable tool for preliminary mooring system assessments.

However, due to the absence of active load mitigation through control mechanisms, the simplified model exhibited a tendency to overpredict responses in certain frequency bands. These discrepancies may lead to conservative or inaccurate assessments in fatigue analysis or detailed structural design, especially in components sensitive to specific dynamic behaviors. In such cases, additional uncertainty analysis or conservative design margins may be required.

Furthermore, the validation presented in this study is limited to DLC 1.2, and for a comprehensive design of the mooring system, it is necessary to analyze a broader range of DLCs, as different load cases may govern the ultimate limit state. Future research is recommended to extend the evaluation of this simplified modeling approach to a wider set of influential design scenarios, including other operational DLCs as well as potential fault or shutdown conditions, to assess its capability in predicting maximum loads. In addition, it would be meaningful to investigate the applicability of the model for estimating fatigue damage contributions and for integration into more extensive extreme value analysis frameworks based on multiple DLC simulations.

Acknowledgement

This research was supported by Korea Institute of Energy Technology Evaluation and Planning (KETEP) grant funded by the Korean government (MOTIE) (20213000000030) Development of disconnectable mooring system for A MW class floating offshore wind turbine.

References

[1] IRENA, 2023, “Offshore Renewables: An Action Agenda for Deployment”, International Renewable Energy Agency.

[2] WindEurope, 2023, “Wind energy in Europe: 2022 statistics and the outlook for 2023-2027”, WindEurope, https://windeurope.org/intelligence-platform/product/wind-energy-in-europe-2022-statistics-and-the-outlook-for-2023-2027/.

[3] Jonkman, J.M., 2007, “Dynamics modeling and loads analysis of an offshore floating wind turbine”, NREL/TP-500-41958, NREL, https://www.nrel.gov/docs/fy08osti/41958.pdf.

[4] Butterfield, S., Musial, W., Jonkman, J., and Sclavounos, P., 2007, “Engineering challenges for floating offshore wind turbines”, NREL/CP-500-38776, NREL, https://docs.nrel.gov/docs/fy07osti/38776.pdf.

[5] Henderson, A.R., and Patel, M.H., 2003, "On the modelling of a floating offshore wind turbine", Wind Energy, **6**(1), 53-86. https://doi.org/10.1002/we.83.

[6] Wang, L., and Sweetman, B., 2012, "Simulation of large-amplitude motion of floating wind turbines using conservation of momentum", Ocean Eng., **42**, 155-164.

[7] Coulling, A.J., Goupee, A.J., Robertson, A.N., Jonkman, J.M., and Dagher, H.J., 2013, "Validation of a FAST semi-submersible floating wind turbine numerical model with DeepCwind test data", J. Renew. Sustain. Energy, **5**(2), 023116. https://doi.org/10.1063/1.4796197.

[8] Karimirad, M., and Moan, T., 2012, "A simplified method for coupled analysis of floating offshore wind turbines", Mar. Struct., **27**(1), 45-63.

[9] Lackner, M.A., and Rotea, M.A., 2011, "Structural control of floating wind turbines", Mechatronics, **21**(4), 704-719. https://doi.org/10.1016/j.mechatronics.2010.11.007.

[10] Jonkman, J.M., and Buhl, M.L., 2005, "FAST user's guide", NREL/EL-500-38230, NREL. https://docs.nrel.gov/docs/fy06osti/38230.pdf.

[11] NREL, 2022, "OpenFAST Documentation", Accessed 11 June 2025, https://openfast.readthedocs.io.

[12] Matha, D., 2010, "Model development and loads analysis of an offshore wind turbine on a TLP", NREL/TP-500-45891, NREL. https://docs.nrel.gov/docs/fy10osti/45891.pdf.

[13] Hall, M., Buckham, B., and Crawford, C., 2014, "Evaluating the importance of mooring line model fidelity in floating offshore wind turbine simulations", Wind Energy, **17**(12), 1835-1853. https://doi.org/10.1002/we.1669.

[14] López-Queija, J., Robles, E., Llorente, J.I., Touzon, I., and López-Mendia, J., 2022, "A simplified modeling approach of floating offshore wind turbines for dynamic simulations", Energies, **15**(6), 2228. https://doi.org/10.3390/en15062228.

[15] Pegalajar-Jurado, A., and Bredmose, H., 2018, "An efficient frequency-domain model for quick load analysis of floating offshore wind turbines (QuLAF)", Wind Energ. Sci., **3**(2), 693-712. https://doi.org/10.5194/wes-3-693-2018.

[16] Bachynski, E.E., and Moan, T., 2012, "Design considerations for tension leg platform wind turbines", Mar. Struct., **29**(1), 89-114. https://doi.org/10.1016/j.marstruc.2012.09.001.

[17] Lerch, M., De-Prada-Gil, M., and Molins, C., 2018. "A simplified model for the dynamic analysis and power generation of a floating offshore wind turbine", E3S Web of Conferences, **61**, 00001. https://doi.org/10.1051/e3sconf/20186100001.

[18] Taruffi, F., Novais, F., and Viré, A., 2024, "An experimental study on the aerodynamic loads of a floating offshore wind turbine under imposed motions", Wind Energ. Sci., **9**(2), 343-358. https://doi.org/10.5194/wes-9-343-2024.

[19] Li, L., Gao, Z., and Moan, T., 2015, "Joint distribution of environmental condition at five European offshore sites for design of combined wind and wave energy devices", J. Offshore Mech. Arct. Eng., **137**(3), 031901. https://doi.org/10.1115/1.4029842.

[20] Gaertner, E., Rinker, J., Sethuraman, L., Zahle, F., Anderson, B., Barter, G., Abbas, N., Meng, F., Bortolotti, P., Skrzypinsk, W., *et al*., 2020, "IEA Wind TCP Task 37: Definition of the IEA 15-Megawatt Offshore Reference Wind Turbine", NREL/TP-5000-75698, NREL. https://www.nrel.gov/docs/fy20osti/75698.pdf.

[21] Allen, C., Viselli, A., Dagher,H., Goupee, A., Gaertner, E., Abbas, N., Hall, M., Barter, G., 2020 "IEA Wind TCP Task 37: Definition of the UMaine VolturnUS-S Reference Platform Developed for the IEA Wind 15-Megawatt Offshore Reference Wind Turbine", NREL/TP-5000-76773, NREL. https://docs.nrel.gov/docs/fy20osti/76773.pdf.

[22] DNV, 2010, "DNV-RP-C205: Environmental Conditions and Environmental Loads", Det Norske Verita.